ACI STRUCTURAL JOURNAL TECHNICAL PAPER

Title no. 109-S08

Shear-Peeling Bond Strength between Continuous Fiber Sheet and Concrete

by M. S. Alam, T. Kanakubo, and A. Yasojima

Diagonal tension cracks in reinforced concrete members may adversely affect the performance of flexurally strengthened members by fiber-reinforced polymer (FRP) materials. The interface between the FRP sheet and concrete may experience both shear bond and peeling for such conditions. This study presents the experimental results of bond strength between the FRP sheet and concrete interface for both shear bond and peeling conditions. Twenty-seven rectangular specimens with FRP sheets bonded on two sides were tested in uniaxial tensile loading. The specimens were designed for different step angles at the middle to ensure that the interface acts for both shear and peeling conditions. Three types of woven composite sheets made of aramid (Aramid 1 and Aramid 2) and carbon were used in this investigation. The three different sheets were chosen to allow various sheet stiffnesses and strengths to be studied. The results revealed that the bond strength decreases considerably due to the peeling effect. In addition, the step angle and fiber stiffness play an important role in the bond strength for a combined effect. The highest bond strength was observed for the lowest axial stiffness of the laminate. Based on the test results, a modification has been proposed to one of the existing bond strength models. The proposed modification improves the prediction of the bond strength between FRP laminate and concrete.

Keywords: bond strength; delamination; fiber-reinforced polymer sheet; interface; tensile load.

INTRODUCTION

The existing concrete structures in service may be deficient in shear capacity or damaged due to improper design of the shear reinforcement, construction faults or poor construction practice, a reduction in the shear reinforcement area due to corrosion, an increase in external loads, or insufficient maintenance, and chemical processes caused by harsh environmental conditions.[1,2]

A large number of new materials and techniques are currently available for structural strengthening and rehabilitation, including external prestressing, adding extra reinforcement by stapling and shotcreting, providing extra support to reduce span length, bonding steel plate by epoxy adhesives,[1] and bonding of composite plates to reinforced and prestressed concrete beams to increase flexural stiffness and strength.[2-12] Among these, external bonding of fiber-reinforced polymer (FRP) sheets has emerged as a popular method for the strengthening or retrofitting of reinforced concrete structures. Many researchers[1-24] have carried out various experiments on concrete structures strengthened with FRP sheets. While a significant amount of research has been conducted on the flexural strengthening of concrete beams with externally applied composite reinforcement,[2-13] some work has also been done on shear strengthening.[1,12-24]

The test results indicate that shear strengthening of beams with externally applied composite materials may provide a significant increase in shear strength.[1,12-24] Chajes et al.[15] reported that externally applied composite fabrics made of aramid, E-glass, and graphite fibers can be used to enhance the shear capacity of concrete beams. An increase in ultimate strength of 60 to 150% was observed in their investigation. In all of these studies, the FRP sheets were considered to act in plane with the member surface, and the interface between the FRP sheet and concrete was subjected to shear bond stress (called Mode II in fracture mechanics). In the case of flexurally strengthened concrete beams, however, when delamination is induced by the opening up (Mode I) of a flexural shear crack and a shear crack, a relative vertical displacement exists between the two sides of the crack. Furthermore, the same situation occurs in the case of punching shear (Fig. 1). In this case, the FRP sheets on one side of the crack are subjected to direct tension and the interface between the FRP sheet and concrete undergoes both interfacial shear and peeling effects (combination of Modes I and II), thus resulting in a reduction of bond strength, which in turn increases the probability of premature local collapse. Hence, the bond performance of this type of structure, strengthened by FRP, depends not only on the shear bond strength of the interface, but also on the combined effect of shear bond and peeling. In evaluating the performance of the externally bonded FRP strengthening technique, the interfacial bond strength between the FRP sheet and concrete in different failure modes is of crucial importance.

Many studies have been carried out to understand the bond characteristics between concrete and FRP in different test conditions (for example, the single shear test,[25,26] the

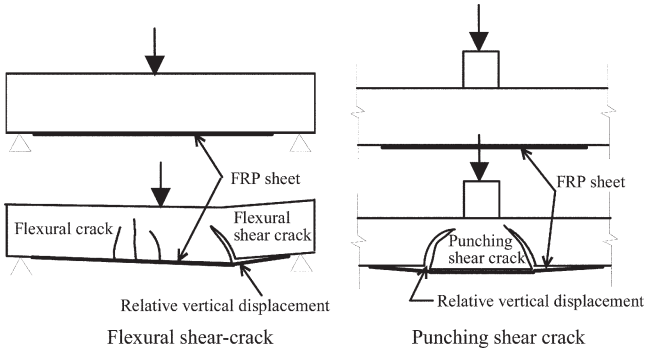

Fig. 1—Relative vertical displacement between two sides of crack.

ACI Structural Journal, V. 109, No. 1, January-February 2012.

M. S. Alam *is a Postdoctoral Fellow in the Faculty of Engineering and Applied Science at Memorial University of Newfoundland, St. John's, NL, Canada. He received his BSc, MEng, and PhD in engineering from Bangladesh University of Engineering and Technology (BUET), Dhaka, Bangladesh; Saitama University, Saitama, Japan; and Memorial University of Newfoundland, St. John's, NL, Canada, respectively. His research interests include the shear behavior of concrete structures reinforced with steel and fiber-reinforced polymer composites, the strengthening and rehabilitation of concrete structures, and finite element analysis of reinforced concrete.*

ACI member **T. Kanakubo** *is an Associate Professor in the Department of Engineering Mechanics and Energy at the University of Tsukuba, Tsukuba, Japan. He received his PhD in engineering from the University of Tsukuba. His research interests include fiber-reinforced concrete, fiber-reinforced polymer for concrete, and the bond mechanism of concrete structures.*

A. Yasojima *is an Assistant Professor in the Department of Engineering Mechanics and Energy at the University of Tsukuba. He received his PhD in engineering from the University of Tsukuba. His research interests include the bond-splitting behavior of reinforced concrete structures.*

double shear test,[27] the direct tensile test,[28] the modified beam test,[29] and the test with curvature in beam[30]). However, the laminate-concrete interface is susceptible to the relative vertical displacement of the shear cracks in the beam.[31] This could lead to the delamination or peeling of the FRP from the concrete. Some authors[3,5,10] have reported that the retrofitted beam can fail due to the failure of the concrete layer between the FRP and steel or due to the delamination or peeling of the FRP from the concrete. Karbhari et al.[32] conducted a pure peeling test to determine the bond strength between the concrete and FRP sheets. Triantafillou and Plevris[33] proposed a model for the peeling of debonding mechanisms. Further investigation is needed to determine the bond strength between the FRP sheet and concrete for combined shear and peeling conditions. Therefore, the objective of this research is to study the interfacial bond strength between FRP sheets and concrete for combined shear and peeling conditions and to observe the influence of the fiber types.

RESEARCH SIGNIFICANCE

FRP sheet bonding has emerged as one of the most promising techniques for the strengthening and repair of structurally deficient members. When there are shear cracks in the members, however, the bond between the FRP sheet and concrete may adversely affect the performance of the strengthened structures. The behavior of the bond between the FRP sheet and concrete, where the FRP sheets are subjected to both axial and shear force, has not yet been fully explored. The purpose of this study is to investigate the bond and effect of fiber stiffness on the behavior of the bond for the combined action of axial and shear force in FRP sheets. This study will help structural engineers and construction practitioners understand the behavior of beams strengthened by FRP sheets with major shear cracks.

EXPERIMENTAL INVESTIGATION

The bond between FRP sheets and concrete was examined experimentally for combined axial and shear conditions. The tests were carried out in uniaxial tension for specimens with FRP sheets bonded on two sides. The details of the experimental program are given in the following sections.

Materials

Three types of fiber sheets—namely, Aramid 1, Aramid 2, and carbon—were used in this study. The width of the sheets was 50 mm (2 in.). The details of the fiber properties obtained from the manufacturer are shown in Table 1. Two batches of concrete with strengths of 18 and 36 MPa (2610 and 5220 psi) were used for this experiment. The details of the concrete properties are shown in Table 2.

Specimens

A total of 27 concrete specimens, with two different cross sections for each specimen to allow for a specified step angle, were prepared to test in uniaxial loading. The cross section for half of the specimen was 100 x 100 mm (4 x 4 in.) and varied for the remaining half. The total length of each specimen was 600 mm (24 in.). FRP sheets were bonded for the total length to allow for a 300 mm (12 in.) bond length on each side. The bond length recommended by previous researchers[34-37] (effective bond length) is approximately 100 mm (4 in.) for plane bonding. Due to the step angle, the bond length used in this investigation was greater than the recommended bond length.

The specimens were reinforced with two φ22 mm (φ7/8 in.) steel bars in the longitudinal direction for clamping and loading. The details of the specimens used in this study are shown in Fig. 2. The variables for all the specimens were the step angles, represented by $\tan\theta_{ini}$, and the fiber types. The values of $\tan\theta_{ini}$ were 0.17, 0.33, 0.5, and 1.0. These

Table 1—Fiber properties

Type of fiber	Fiber strength	Fiber thickness, mm	Tensile strength, MPa	Elastic modulus, GPa	Tensile stiffness, kN/mm
Aramid 1	600 kN/m	0.286	2060	118	33.7
	1200 kN/m	0.572	2060	118	67.5
Aramid 2	600 kN/m	0.252	2350	78	19.8
Carbon	300 g/m^2	0.167	3500	230	38.4

Notes: 1 mm = 0.0394 in.; 1 MPa = 145 psi; 1 GPa = 145 ksi; 1 kN/m = 5.69 lb/in.; 1 kN/mm = 5.69 kip/in.; 1 g/m^2 = 1.42 × 10^{-6} lb/in.^{2}

Table 2—Concrete properties

Batch No.	Specimen ID	Compressive strength, MPa	Splitting strength, MPa	One-third secant modulus, GPa
1	A106-15,30 A112-15,30 A206-15 C300-15	20.6	2.26	19.9
2	A106-05,10 A206-05	37.3	2.74	25.0

Notes: 1 MPa = 145 psi; 1 GPa = 145 ksi.

variations in step angles were made within 30 mm (1.2 in.) at the center.

The specimens were prepared in two stages. The concrete prisms were cast and cured for 28 days. Two surfaces of the prisms were then smoothed by a disk sander to apply the FRP sheets. The primer was applied on the treated surface by using a hard rubber roller. After the primer cured, putty was applied. Epoxy resin was applied on the putty and the FRP sheet was positioned with the application of slight pressure to impregnate all the fibers in the resin. Finally, another layer of resin was applied on the sheet. After reinforcing by FRP sheets, the specimens were cracked at the center using a hammer on the notch. The two steel bars had no connections and the two prisms were connected through the FRP sheets.

One of the ends of the specimen was confined by transverse FRP sheets wrapped around all four sides to force a debonding of the sheet only on the opposite end where the strain gauges were set. Three specimens were made for each combination of step angle and fiber. The identification of the specimens is shown in Fig. 3. Concrete cylinders were cast from the same batch of concrete and cured under the same laboratory conditions as the specimens. The cylinders were tested at the same time when the specimens were tested to determine the material properties.

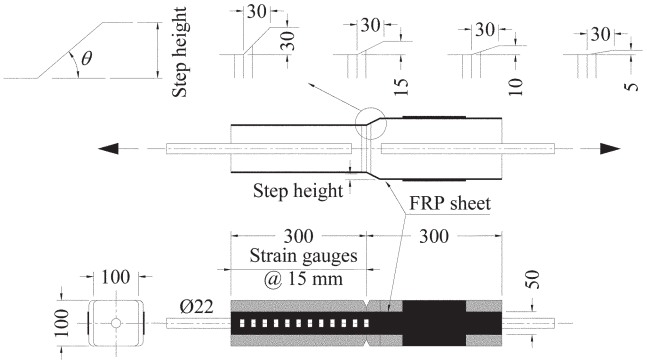

Fig. 2—Specimen details. (Note: 1 mm = 0.0394 in.)

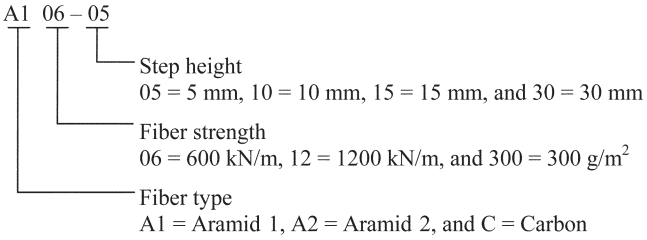

Fig. 3—Specimen identification. (Note: 1 mm = 0.0394 in.; 1 kN/m = 5.69 lb/in.; 1 g/m^2 = 1.42 × 10^{-6} lb/in.^{2})

Test setup and procedure

All the specimens were subjected to tensile force by a universal testing machine, causing shear and peeling debonding at the interface, as shown in Fig. 4. For each combination of test variables, one specimen was instrumented with 15 strain gauges on the FRP sheet on one side of the specimen. These gauges were spaced at 15 mm (0.6 in.) from the center of the specimen. On the opposite side, one gauge was used at the center of the specimen. For the remaining two specimens of each set, two strain gauges were attached on two sides at the center of the specimen. The total displacement and crack width at the center were measured by using linear variable displacement transducers (LVDTs).

TEST RESULTS AND DISCUSSION

Failure progress

The experimental results are shown in Table 3. All the specimens were subjected to tensile force until failure on either side. The load-displacement (crack width) curve is shown in Fig. 5. It can be seen that an almost identical

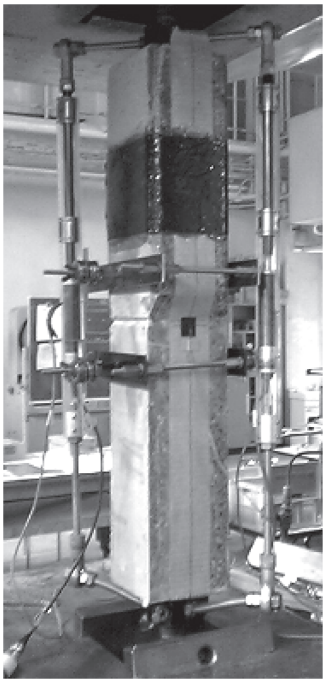

Specimen in loading frame

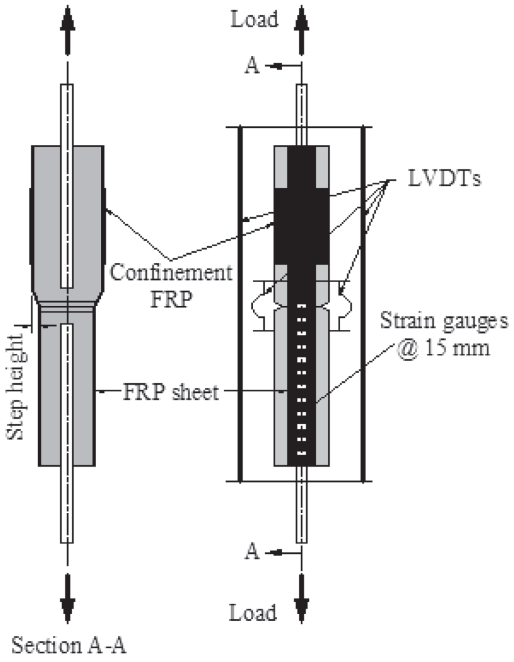

Fig. 4—Test setup. (Note: 1 mm = 0.0394 in.)

Table 3—Experimental results

Specimen ID		Step angle $\tan\theta_{ini}$	Maximum load P_{max}, kN	Bond strength $P = P_{max}/2$, kN	Calculated bond strength[38] P_{cal}, kN	P/P_{cal}
A106-05	1	0.17	23.23	11.62	12.23	0.95
	2		18.47	9.24		0.75
	3		22.58	11.29		0.92
A106-10	1	0.33	16.66	8.33	12.23	0.68
	2		13.80	6.90		0.56
	3		12.55	6.28		0.51
A106-15	1	0.50	17.20	8.60	11.53	0.75
	2		16.11	8.05		0.70
	3		16.67	8.34		0.72
A106-30	1	1.0	9.00	4.50	11.53	0.39
	2		11.24	5.65		0.49
	3		9.00	4.50		0.39
A112-15	1	0.5	17.30	8.65	16.31	0.53
	2		16.08	8.04		0.49
	3		18.79	9.40		0.58
A112-30	1	1.0	11.19	5.60	16.31	0.34
	2		10.68	5.34		0.33
	3		9.25	4.63		0.28
A206-05	1	0.17	18.02	9.01	9.14	0.99
	2		17.16	8.58		0.94
	3		17.01	8.51		0.93
A206-15	1	0.5	16.87	8.44	8.61	0.98
	2		16.85	8.43		0.98
	3		15.06	7.53		0.87
C300-15	1	0.5	13.34	6.67	10.21	0.65
	2		15.56	7.78		0.76
	3		15.74	7.87		0.77

Note: 1 kN = 0.2248 kips.

load-displacement curve was observed for three repeating specimens (Fig. 5(a)). Similarly, the differences between the load-displacement curves for different FRP types for the same step angle are negligible (Fig. 5(d)). This indicates that the load-displacement curve does not change with the change in FRP stiffness. On the other hand, significant differences were observed for different step angles. For the same load level, the displacement increases as the step angle increases for all FRP types. A decrease in the step angle is associated with an increase in the observed displacement. Sudden drops in the load represent the propagation of delamination. As expected, more pronounced displacement is observed for Specimen A106-30 due to the large step angle. Figure 6 shows a typical photograph of a specimen after failure. From the post-failure photograph, it is apparent that some concrete is attached at the end region of the sheet, which could be due to the shearing between the FRP laminate and concrete. On the other hand, no concrete is attached at the region adjacent to the step. This could be due to the peeling of the sheet near the center of the specimen where the step angle is applied.

FRP strain distribution

The observed strain distribution, along with the tensile force versus crack width diagrams for some specimens, are shown in Fig. 7. During loading, the strain in FRP near the step angle increases as the load increases. Just before the delamination of the interface, however, a negative strain was observed in the strain gauge near the step, caused by bending in the FRP. As the delamination progressed, this behavior was propagated for different strain gauges. For the strain gauges located far from the center of the specimen, a decrease in strain value was observed instead of a negative strain. This could be attributed to the fact that, to delaminate the FRP laminate far from the center, the load should be increased. This increase in load may cause a higher tensile strain in the FRP than its compressive strain due to bending. After delamination, the FRP strain begins to increase. This phenomenon is observed for almost all of the strain gauges located at 15 mm (0.6 in.) intervals. Several strain distributions are shown in Fig. 7 for specific crack widths, as marked on the tensile force versus crack widths diagram. Due to the increase in load and corresponding crack width, the reduction in the FRP strain moves from the center of the

specimen toward the end, where delamination of the FRP sheet was observed at failure.

Bond strength evaluation

Kanakubo et al.[38] proposed a model to calculate the bond strength between the FRP laminate and concrete without any step angle. To investigate the effect of the step angle on this model, the experimental bond strength is normalized by the calculated bond strength using the model. According to Kanakubo et al.,[38] the bond strength P_b is given by the following equation

$$\begin{aligned} P_b &= 1.1 f_c'^{\,0.2} b_f l_e && (l_b \geq l_e) \\ P_b &= \left\{ 0.7\cos\left(\frac{l_b}{l_e}\right)\pi + 1.8 \right\} f_c'^{\,0.2} b_f l_b && (l_b < l_e) \end{aligned} \quad (1)$$

where l_e is the effective bond length = $0.7\sqrt{t_f E_f / f_c'^{0.2}}$; t_f is the thickness of the fiber; E_f is the elastic modulus of the fiber; f_c' is the concrete compressive strength; b_f is the fiber width; and l_b is the bond length.

The normalized bond strengths are plotted against the fiber types in Fig. 8. The data indicate that the normalized bond strength of Specimen A112 is less than that of A106, whereas the fiber stiffness of A112 is greater than that of A106. Again, the stiffness of A206 is less than the stiffness of A106 and the bond strength is larger than that of A106. Hence, the data indicate that the bond strength increases with a decrease in fiber stiffness. This can be attributed to the fact that the higher stiffness of the FRP laminate is more prone to the peeling effect. Conversely, an increase in the step angle resulted in an observed decrease in bond strength. This phenomenon is observed for different fiber types. Hence, it can be concluded that the bond strength decreases with the increase in the step angle, irrespective of the fiber type.

A detailed delamination process is shown in Fig. 9. As the load increases, the delamination of the sheet occurs due to the peeling effect. Simultaneously, the bond length and the angle (tanθ) between the fiber and the concrete face decreases. The delaminated region is defined as the distance from the center of the specimen to the strain gauges where the maximum negative strain is observed. The rest of the fiber sheet is the bonded region, which gradually diminishes at failure. As shown in Fig. 7, the step angle can be calculated by dividing the step height by the distance of the strain gauges from the center for which the negative strain has occurred. The load P corresponding to this negative strain was recorded from the data. The ratio of this tensile load P with the calculated bond strength P_{cal} using Eq. (1) is plotted against the step angle (tanθ) in Fig. 10 for some specimens. It can be seen that the tensile load decreases exponentially with the increase in the step angle. Due to the increase in the step angle, however, the tensile load asymptotically approaches the peeling strength of the interface. As previously stated, for the case of decreasing the step angle, the tensile load increases and approaches the shear bond strength. The center portion of the curve governs for the combined shear-peeling conditions. Consequently, the normalized bond length decreases exponentially with the decrease in the step angle, indicating that the delamination of the interface is a nonlinear process.

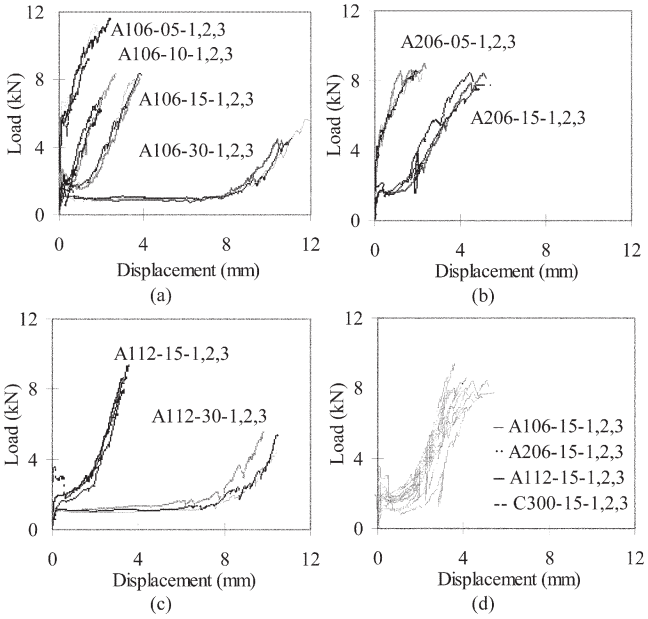

Fig. 5—Load-displacement curve: (a) Specimen A106; (b) Specimen A206; (c) Specimen A112; and (d) for different specimens with same step angle. (Note: 1 kN = 0.2248 kips; 1 mm = 0.0394 in.)

← *loading end* *step* →

Fig. 6—Typical failure surface for concrete and fiber.

The trend line of the behavior of the bond strength (shear-peeling conditions) for the A106 series of specimens can be represented by the following equation

$$y = ax^b \quad (2)$$

where $y = P/P_{cal}$; $x = \tan\theta$; $a = 0.053$; and $b = -0.77$, as shown in Fig. 10. A plot of this equation, together with the proposed model by Kanakubo et al.,[38] is shown in Fig. 11. The intersection of these plots is within the shear-peeling zone. As can be seen in Fig. 10, the intersection point moves with the change in the step angle and, thus, there will be different values for each specimen. Using the values of P/P_{cal} of these intersections, the corresponding values of tanθ were calculated from Eq. (2). Once the value of tanθ is known, the bond length can be calculated using the step height. The values of P/P_{cal} and tanθ and the calculated bond length for each specimen are tabulated in Table 4. It appears that the bond length decreases with the increase in the step angle. Finally, the bond strength for the specimens with step angles was obtained using the modification factor on the right-hand

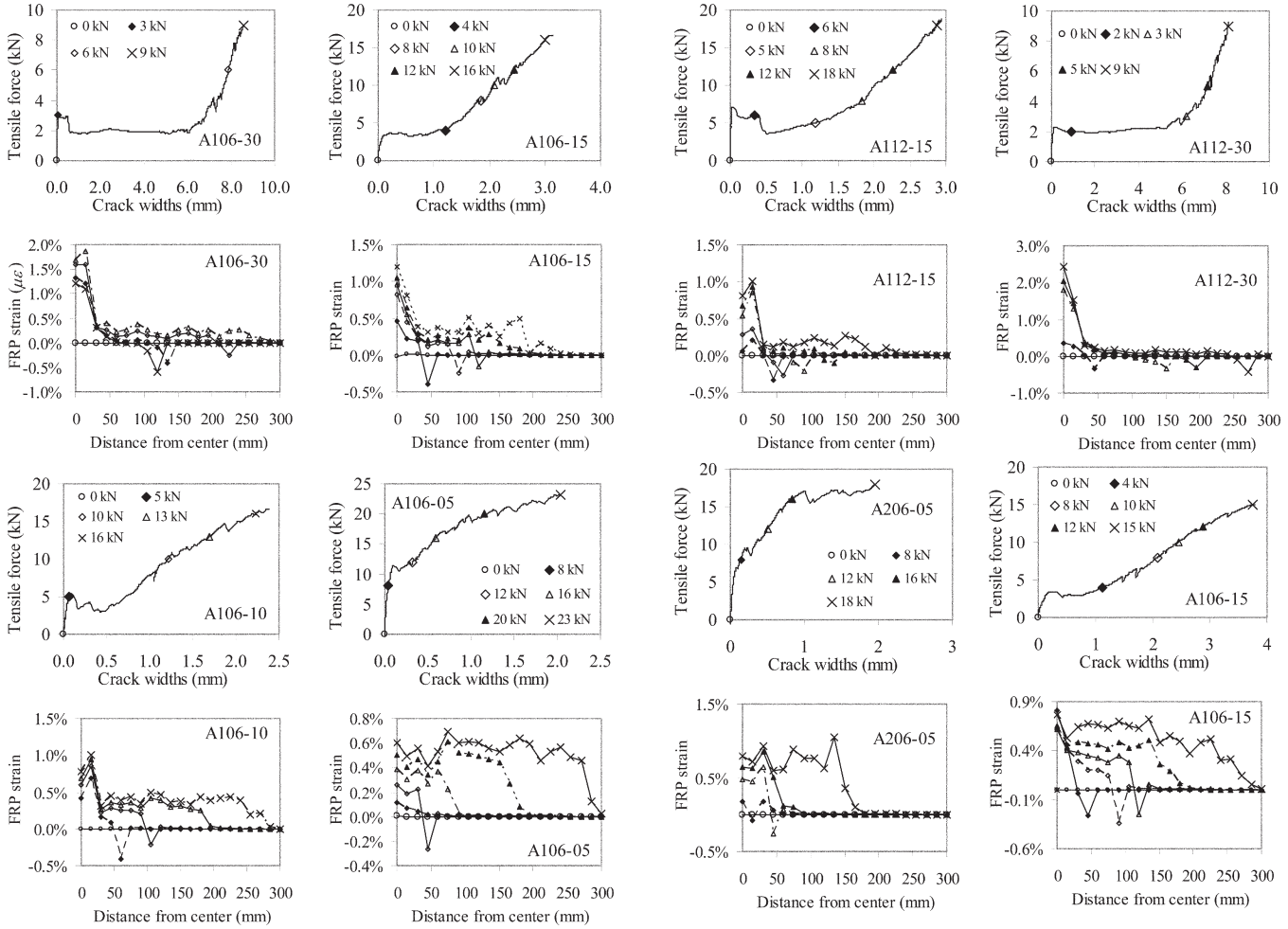

Fig. 7—Strain distribution in FRP. (Note: 1 kN = 0.2248 kips; 1 mm = 0.0394 in.)

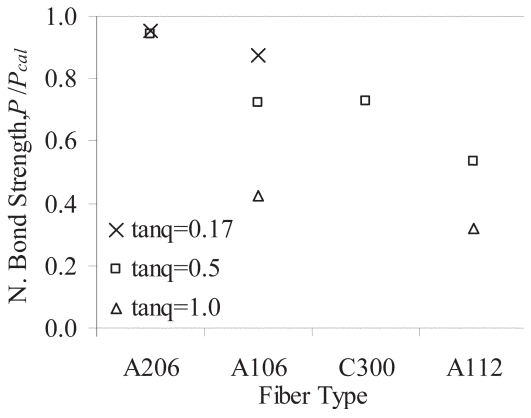

Fig. 8—Effect of fiber types on bond strength.

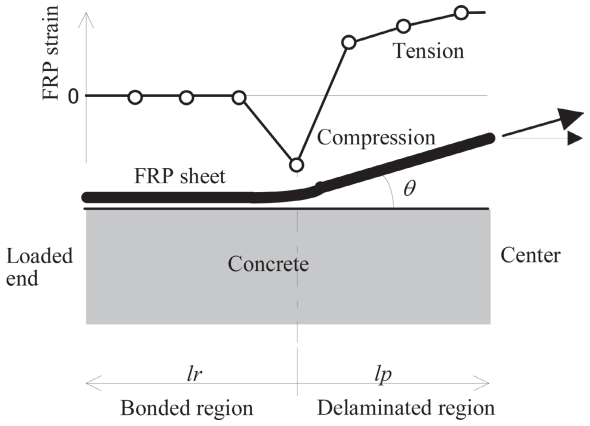

Fig. 9—Details of delamination process.

side of Eq. (2) into Eq. (1). The comparison between these bond strengths and those obtained from the test results is shown in Table 4. It can be seen that the predictions are better than those using Eq. (1).

CONCLUSIONS

The bond strength between the FRP sheet and concrete interface for combined shear and peeling conditions is greatly influenced by the step angles and fiber stiffness. It decreases exponentially as the step angle increases. Therefore, in calculating the bond length and strength, possible level differences between the strengthened surfaces adjacent to a crack should be considered. It was also observed that the bond strength increases with the decrease in the fiber stiffness. Based on the test results, a modification of the existing model of Kanakubo et al.[38] has been proposed. The proposed modification improves the prediction of the bond strength between FRP laminate and concrete for shear-peeling conditions.

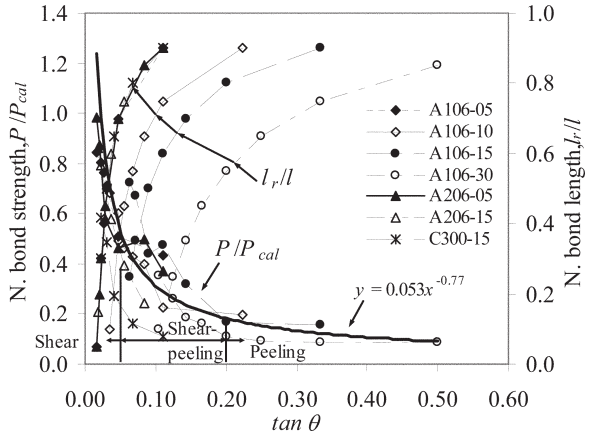

Fig. 10—Effect of step angles on bond strength.

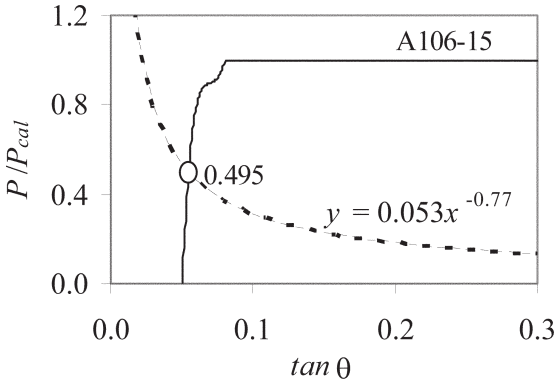

Fig. 11—Typical plot of proposed equation with Kanakubo et al.[38]

Table 4—Calculated results for different specimens

Specimen	Calculated bond length, mm	P/P_{cal}	tanθ	New P_{cal} (Eq. (2)), kN	P/P_{cal} (Eq. (2))
A106-05	57.84	0.854	0.021	12.7	0.84
A106-10	31.55	0.607	0.037	8.2	0.87
A106-15	25.37	0.485	0.055	5.7	1.45
A106-30	16.58	0.330	0.106	3.4	1.42
A112-15	35.05	0.475	0.057	7.8	1.11
A112-30	23.11	0.325	0.108	4.8	1.08
A206-05	47.67	0.875	0.020	9.8	0.89
A206-15	19.22	0.491	0.053	4.4	1.86
C300-15	22.62	0.487	0.054	5.1	1.45

Notes: 1 mm = 0.0394 in.; 1 kN = 0.2248 kips.

REFERENCES

1. Al-Sulaimani, G. J. et al., "Shear Repair for Reinforced Concrete by Fiberglass Plate Bonding," *ACI Structural Journal*, V. 91, No. 3, May-June 1994, pp. 458-464.

2. Capozucca, R., and Cerri, M. N., "Static and Dynamic Behavior of RC Beam Model Strengthened by CFRP-Sheets," *Construction and Building Materials*, V. 16, 2002, pp. 91-99.

3. Ritchie, P. A.; Thomas, D. A.; Lu, L. W.; and Connelly, G. M., "External Reinforcement of Concrete Beams Using Fiber Reinforced Plastics," *ACI Structural Journal*, V. 88, No. 4, July-Aug. 1991, pp. 490-500.

4. Reed, M. W.; Barnes, R. W.; Schindler, A. K.; and Lee, H. W., "Fiber-Reinforced Polymer Strengthening of Concrete Bridges that Remain Open to Traffic," *ACI Structural Journal*, V. 102, No. 6, Nov.-Dec. 2005, pp. 823-831.

5. Sharif, A. et al., "Strengthening of Initially Loaded Reinforced Concrete Beams Using FRP Plates," *ACI Structural Journal*, V. 91, No. 2, Mar.-Apr. 1994, pp. 160-168.

6. Takeda, K. et al., "Flexural Behavior of Reinforced Concrete Beams Strengthened with Carbon Fiber Sheets," *Composites Part A*, V. 27A, 1996, pp. 981-987.

7. Arduini, M., and Nanni, A., "Behavior of Precracked RC Beams Strengthened with Carbon FRP Sheets," *Journal of Composites for Construction*, ASCE, V. 1, No. 2, 1997, pp. 63-70.

8. Saeed, A.; Saha, A.; and Nadar, A., "Strengthening and Rehabilitation of Concrete Structures with Carbon Fiber Reinforced Polymers (CFRP)," *Earth & Space 2006: Proceedings of the Tenth Biennial ASCE Aerospace Division International Conference on Engineering, Construction, and Operations in Challenging Environments*, ASCE, Houston, TX, Mar. 5-8, 2006, pp. 1-8.

9. Grace, N. F.; Sayed, G. A.; Soliman, A. K.; and Saleh, K. R., "Flexure-Strengthening Reinforced Concrete Beams Using Fiber Reinforced Polymer (FRP) Laminates," *ACI Structural Journal*, V. 96, No. 5, Sept.-Oct. 1999, pp. 865-875.

10. Saadatmanesh, H., and Ehsani, M. R., "RC Beams Strengthened with GFRP Plates. I: Experimental Study," *Journal of Structural Engineering*, ASCE, V. 117, No. 11, 1991, pp. 3417-3433.

11. Lorenzis, L. D.; Miller, B.; and Nanni, A., "Bond of Fiber-Reinforced Polymer Laminates to Concrete," *ACI Materials Journal*, V. 98, No. 3, May-June 2001, pp. 256-264.

12. Garden, H. N., and Hollaway, L. C., "An Experimental Study of Influence of Plate End Anchorage of Carbon Fiber Composite Plates Used to Strengthen Reinforced Concrete Beams," *Composite Structures*, V. 42, 1998, pp. 175-188.

13. Norris, T.; Saadatmanesh, H.; and Eshani, M. R., "Shear and Flexural Strengthening of RC Beams with Carbon Fiber Sheet," *Journal of Structural Engineering*, ASCE, V. 123, No. 7, 1997, pp. 903-911.

14. Triantafillou, T. C., "Shear Strengthening of Reinforced Concrete Beams Using Epoxy-Bonded FRP Composites," *ACI Structural Journal*, V. 95, No. 2, Mar.-Apr. 1998, pp. 107-115.

15. Chajes, M. J. et al., "Shear Strengthening of Reinforced Concrete Beams Using Externally Applied Composite Fabrics," *ACI Structural Journal*, V. 92, No. 3, May-June 1995, pp. 295-303.

16. Khalifa, A., and Nanni, A., "Rehabilitation of Rectangular Simply Supported RC Beams with Shear Deficiencies Using CFRP Composite," *Construction and Building Materials*, V. 16, 2002, pp. 135-146.

17. Dolan, C. W.; Rider, W.; Chajes, M. J.; and DeAscanis, M., "Prestressed Concrete Beams Using Non-Metallic Tendons and External Shear Reinforcement," *Fiber-Reinforced-Plastic Reinforcement for Concrete Structures—International Symposium*, SP-138, A. Nanni and C. W. Dolan, eds., American Concrete Institute, Farmington Hills, MI, 1993, pp. 475-496.

18. Adhikary, B. B.; Mutsuyoshi, H.; and Ashraf, M., "Shear Strengthening of Reinforced Concrete Beams Using Fiber-Reinforced Polymer Sheets with Bonded Anchorage," *ACI Structural Journal*, V. 101, No. 5, Sept.-Oct. 2004, pp. 660-668.

19. Bousselham, A., and Chaallal, O., "Shear Strengthening of Reinforced Concrete Beams with Fiber-Reinforced Polymer: Assessment of Influencing Parameters and Required Research," *ACI Structural Journal*, V. 101, No. 2, Mar.-Apr. 2004, pp. 219-227.

20. Bousselham, A., and Chaallal, O., "Behavior of Reinforced Concrete T-Beams Strengthened in Shear with Carbon Fiber-Reinforced Polymer—

An Experimental Study," *ACI Structural Journal*, V. 103, No. 3, May-June 2006, pp. 339-347.

21. Chaallal, O.; Nollet, M. J.; and Perraton, D., "Shear Strengthening of RC Beams by Externally Bonded Side CFRP Strips," *Journal of Composites for Construction*, ASCE, V. 2, No. 2, 1998, pp. 111-113.

22. Teng, S. et al., "Performance of Strengthened Concrete Deep Beams Predamaged in Shear," *ACI Structural Journal*, V. 93, No. 2, Mar.-Apr. 1996, pp. 159-171.

23. Arduini, M.; Antonio, A.; and Romagnolo, M., "Performance of One-Way Reinforced Concrete Slabs with Externally Bonded Fiber-Reinforced Polymer Strengthening," *ACI Structural Journal*, V. 101, No. 2, Mar.-Apr. 2004, pp. 193-201.

24. Pellegrino, C., and Modena, C., "Fiber-Reinforced Polymer Shear Strengthening of Reinforced Concrete Beams: Experimental Study and Analytical Modeling," *ACI Structural Journal*, V. 103, No. 5, Sept.-Oct. 2006, pp. 720-728.

25. Yao, J.; Teng, J. G.; and Chen, J. F., "Experimental Study on FRP-to-Concrete Bonded Joints," *Composites. Part B, Engineering*, V. 36, 2005, pp. 99-113.

26. Chajes, M. J.; Finch, W. W.; Januszka, T. F.; and Thomson, T. A., "Bond and Force Transfer of Composite Material Plates Bonded to Concrete," *ACI Structural Journal*, V. 92, No. 3, May-June 1996, pp. 208-217.

27. Hiroyuki, Y., and Wu, Z., "Analysis of Debonding Fracture Properties of CFS Strengthened Member Subjected to Tension," *Proceedings of the Third International Symposium on Non-Metallic (FRP) Reinforcement for Concrete Structures*, Japan Concrete Institute, Sapporo, Japan, Oct. 14-16, 1997, pp. 287-294.

28. Nakaba, K.; Kanakubo, T.; Furuta, T.; and Yoshizawa, H., "Bond Behavior between Fiber-Reinforced Polymer Laminates and Concrete," *ACI Structural Journal*, V. 98, No. 3, May-June 2001, pp. 359-367.

29. Van Gemert, D. A., "Force Transfer in Epoxy-Bonded Steel-Concrete Joints," *International Journal of Adhesion and Adhesives*, V. 1, 1980, pp. 67-72.

30. Aiello, M. A.; Galati, N.; and La Tegola, A., "Effect of Curvature on the Bond between Concrete and CFRP Sheets," *Proceedings of the International Conference on Advanced Polymer Composites for Structural Applications in Construction*, Southampton, UK, Apr. 15-17, 2002, pp. 69-76.

31. Meier, U., "Carbon Fiber Reinforced Polymers: Modern Materials in Bridge Engineering," *Structural Engineering International*, V. 2, No. 1, Feb. 1992, pp. 7-12.

32. Karbhari, V. M.; Engineer, M.; and Eckel II, D. A., "On the Durability of Composite Rehabilitation Schemes for Concrete: Use of a Peel Test," *Journal of Materials Science*, V. 32, No. 1, 1997, pp. 147-156.

33. Triantafillou, T. C., and Plevris, N., "Strengthening of RC Beams with Epoxy-Bonded Fiber-Composites Materials," *Materials and Structures*, V. 25, 1992, pp. 201-211.

34. Horiguchi, T., and Saeki, N., "Effect Test Method and Quality of Concrete on Bond Strength of CFRP Sheet," *Proceedings of the Third International Symposium on Non-Metallic (FRP) Reinforcement for Concrete Structures*, Japan Concrete Institute, Sapporo, Japan, Oct. 14-16, 1997, pp. 265-270.

35. Okano, M. et al., "Carbon Fiber Retrofit of Railway Viaducts Columns," *Proceedings of the Third International Symposium on Non-Metallic (FRP) Reinforcement for Concrete Structures*, Japan Concrete Institute, Sapporo, Japan, Oct. 14-16, 1997, pp. 403-410.

36. Maeda, T. et al., "A Study on Bond Mechanism of Carbon Fiber Sheet," *Proceedings of the Third International Symposium on Non-Metallic (FRP) Reinforcement for Concrete Structures*, Japan Concrete Institute, Sapporo, Japan, Oct. 14-16, 1997, pp. 279-286.

37. Sato, Y.; Kimura, K.; and Kobatake, Y., ""Bond Behavior between CFRP Sheet and Concrete (Part 1)," *Journal of Structural and Construction Engineering*, V. 500, 1997, pp. 75-82. (in Japanese)

38. Kanakubo, T.; Furuta, T.; and Fukuyama, H., "Bond Strength between Fiber-Reinforced Polymer Laminates and Concrete," *Proceedings of the Sixth International Symposium on FRP Reinforcement for Concrete Structures (FRPRCS-6)*, Singapore, July 8-10, 2003, pp. 13-142.